RECENT DEVELOPMENTS IN THE THEORY OF ATMOSPHERIC ROTORS

BY JAMES D. DOYLE AND DALE R. DURRAN

The Sierra Nevada Range is one of the most prominent and steepest mountain barriers in the United States and, not surprisingly, is a well-known location for a multitude of topographically forced atmospheric phenomena. As the prevailing westerly winds pass over the Sierra Nevada, gravity waves are frequently generated. Occasionally these mountain waves result in spectacular topographically forced phenomena such as trapped lee waves, downslope windstorms, rotors, and attendant wave and rotor cloud structures, as shown in the examples in Fig. 1. In situations such as those shown in Fig. 1, severe downslope winds near the surface, sometimes in excess of 50 m s^{-1}, decelerate rapidly in the lee and give way to a return flow back toward the mountain crest that is the lower branch of an intense horizontal circulation, as illustrated in the schematic in Fig. 2. These horizontal vortices, known as rotors, are common to the steep eastern slopes of the Sierra Nevada, and particularly over the Owens Valley, where they are notorious for their intensity (e.g., Whelan 2000). Rotors have also

ROBERT SYMONS

T. HENDERSON

FIG. 1. Photographs over the Owens Valley in the lee of the Sierra Nevada Range, taken during the Sierra Wave Project, illustrating (a) and (b) common rotor characteristics such as rotor and lenticular clouds and (a) blowing dust. The flow in both photographs is from right to left as viewed from the north.

AFFILIATIONS: DOYLE—Naval Research Laboratory, Monterey, California; DURRAN—University of Washington, Seattle, Washington
CORRESPONDING AUTHOR: James D. Doyle, Naval Research Laboratory, Marine Meteorology Division, 7 Grace Hopper Avenue, Monterey, CA 93943-5502
E-mail: doyle@nrlmry.navy.mil
DOI: 10.1175/BAMS-85-3-337
©2004 American Meteorological Society

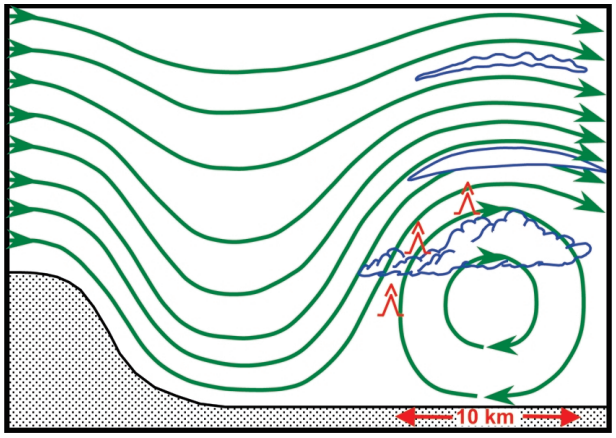

Fig. 2. Schematic streamlines illustrating a rotor circulation and attendant cloud features (adapted from Ludlam and Scorer 1957). Regions of clear-air turbulence associated with the rotor circulation are denoted by the red symbols.

been observed in a number of other mountainous regions, including the Rockies (Lester and Fingerhut 1974) and various locations in Europe (e.g., Queney et al. 1960). Rotors can be severe aeronautical hazards and have been cited as contributing to numerous aircraft encounters with severe turbulence and accidents, including occurrences involving modern commercial and military aircraft. Rotor circulations may also be important for the lifting and transport of aerosols and contaminants, as apparent in Fig. 1a.

Mountain waves and rotors were the subject of one of the first modern U.S. multiagency field programs in meteorology, the Sierra Wave Project (Holmboe and Klieforth 1957; Grubišić and Lewis 2004, personal communication) that took place in the early 1950s (during which the photographs in Fig. 1 were taken). Although research on mountain waves and related phenomena has been very active in the 50 years since the Sierra Wave Project, little attention has been devoted to rotors. Furthermore, there have been almost no thorough observations of real-world rotors because they are dangerous to sample using in situ aircraft measurements, and their small spatial scale prevents them from being resolved by conventional observing networks. Therefore, it is not surprising that mountain-induced rotors still remain poorly understood and difficult to forecast. Only recently have computational resources been sufficient to enable what are thought to be the first realistic numerical simulations of rotors. Here we present results from a high-resolution nonhydrostatic mesoscale model, the Coupled Ocean–Atmosphere Mesoscale Prediction System (COAMPS™; Hodur 1997), which provides a fresh perspective on the structure and characteristics of mountain-induced rotors.

Numerical simulations have suggested that a key aspect of rotor development involves the synergistic interaction between the lee wave and boundary layer effects as discussed recently in Doyle and Durran (2002). As an example, consider the two-dimensional numerical simulation of flow over bell-shaped topography shown in Fig. 3, which is initialized based on a blend of the potential temperature and cross-mountain wind components observed in the Grand Junction, Colorado; Denver, Colorado; and Lander, Wyoming, soundings at 1200 UTC 3 March 1991. On this day, strong winds were observed on the lee side of the Colorado Front Range and rotor clouds were reported at the U.S. Air Force Academy in Colorado Springs, Colorado, between 1355 and 1555 UTC. The horizontal resolution of these simulations is 100 m with 95 vertical levels spanning the interval $0 \leq z \leq 11.6$ km. The details of the model configuration are described by Doyle and Durran (2002). After 3 h of model integration, a series of trapped lee waves has developed in the streamline field with trough-to-crest ampli-

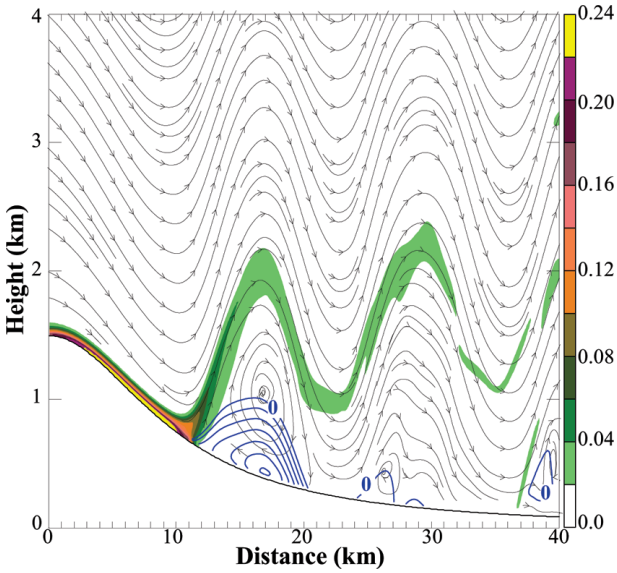

Fig. 3. Streamlines and horizontal vorticity (*y*-component) from a two-dimensional numerical simulation initialized based on a sounding representative of the conditions in central Colorado at 1200 UTC 3 Mar 1991. The cross-mountain wind speed less than or equal to zero is shown using blue isotachs (every 1 m s^{-1}). The horizontal vorticity greater than 0.02 s^{-1} is shaded in color. (From Doyle and Durran 2002.)

tudes exceeding 1200 m. Intense downslope winds, with a maximum of 25 m s^{-1}, develop along the lee slope. Regions of reversed cross-mountain winds associated with a series of rotors are present near the surface beneath the crests of the first three waves. The first rotor downstream of the ridgeline is associated with a maximum reversed cross-mountain wind component of 5.9 m s^{-1} and a region of recirculating flow that extends above the mountain crest. A sheet of y-component vorticity ($\partial u/\partial x - \partial w/\partial z$) originates in the region of high shear within the boundary layer, which forms due to surface friction processes along the lee slope. The vortex sheet separates from the surface, ascends into the crest of the first lee wave, and remains aloft as it is advected downstream by the undulating flow in the lee waves. Boundary layer separation is facilitated by the adverse pressure gradients associated with trapped mountain lee waves. Vertical and horizontal wind shear and turbulence production are maximized along the elevated sheet of horizontal vorticity, particularly along the leading edge of the rotor circulation (as shown schematically in Fig. 2), in general agreement with anecdotal evidence from the Sierra Wave Project (Holmboe and Klieforth 1957) and aircraft observations of rotors taken in the lee of the Rocky Mountain Front Range analyzed by Lester and Fingerhut (1974).

Boundary-layer processes are of fundamental importance in determining rotor development and intensity. For example, an otherwise identical simulation to that shown in Fig. 3, in which a free-slip lower boundary condition was applied, failed to produce rotors or reversed flow. Transient rotors can be generated in the presence of a free-slip lower boundary using a highly idealized upstream sounding, but realistic rotors with characteristics similar to those found in nature appear to develop only in the presence of surface friction. A series of experiments conducted by Doyle and Durran (2002) indicate that an increase in the surface roughness beyond a small value weakens the reversed flow and decreases the depth of the rotor circulation. The surface roughness also has an influence on the downstream location of the rotor because of the impact of the lee wave pressure perturbations on the boundary layer separation. An asymmetry in the solar radiation reaching the ground commonly occurs in mountain-wave events because of the presence of foehn clouds upstream, while the lee slope remains predominantly cloud free. An additional set of simulations was conducted that indicate increasing the lee-side heat flux deepens the rotor circulation, in general agreement with observations taken during the Sierra Wave Project (Kuettner 1959). The turbulence intensity within the rotor also increases due to the contribution of heating from the surface.

In order to examine the dependence of the rotor characteristics on the lee-wave amplitude, Doyle and Durran (2002) conducted an additional series of simulations that were performed with an atmospheric structure in which the upstream static stability is constant throughout each of two horizontal layers. These simulations used varying mountain heights and interface depths to examine a portion of the parameter space relevant to basic rotor dynamics. The results indicate that the magnitude of the reversed flow in the primary rotor for a simulation with surface friction is highly correlated with the strength of the adverse pressure gradient in the primary lee wave in an otherwise identical simulation without surface friction (i.e., with a free-slip lower boundary condition). These simulations also show that, even with surface friction, no rotors form unless the adverse pressure gradient in the corresponding free-slip simulation exceeds a threshold value, further demonstrating synergistic coupling between boundary layer induced vorticity and lee-wave-induced adverse pressure gradients in the formation of low-level rotors.

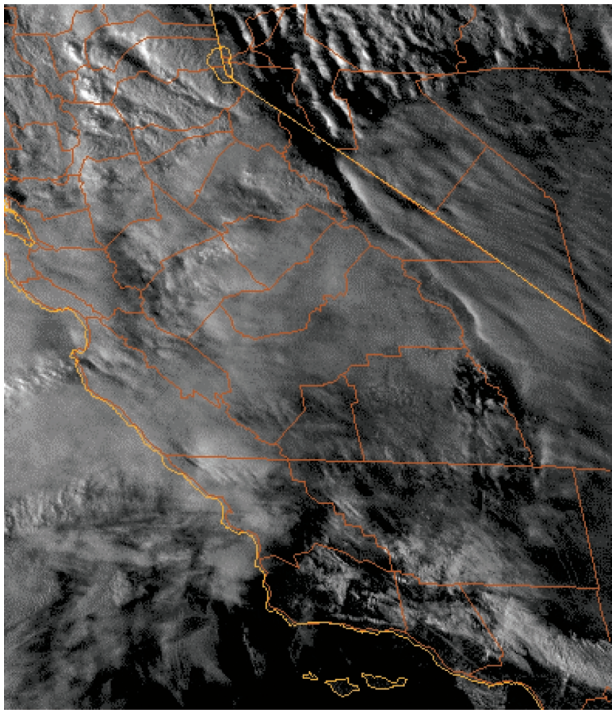

Fig. 4. GOES visible satellite image valid at 0000 UTC 29 October 2000.

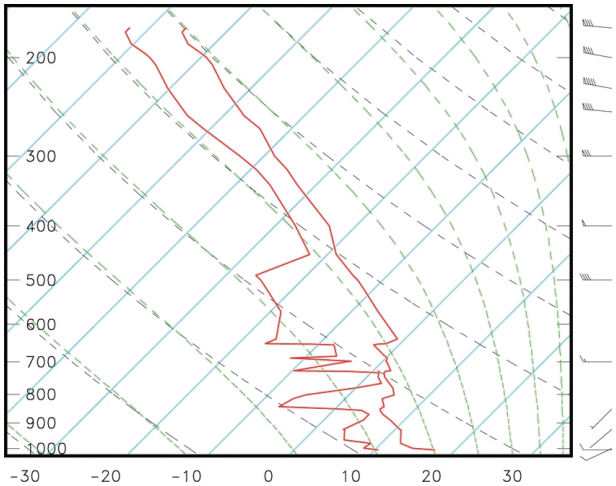

Fig. 5. Skew*T*/log-*P* thermodynamic sounding for Vandenberg, CA, for 0000 UTC 29 October 2000. The horizontal wind speed (m s^{-1}) and direction are shown to the right. One full wind barb corresponds to 5 m s^{-1} and a flag denotes 25 m s^{-1}.

signature of a single stationary wave to the south. A sounding from Vandenberg, California, located approximately 150 km upstream of the Sierra Nevada, at 0000 UTC 29 October 2000 is shown in Fig. 5. The sounding and the larger-scale COAMPS simulation suggest that strong cross-mountain flow (10–15 m s^{-1} at 700 hPa and 20–25 m s^{-1} at 500 hPa) and an inversion near the elevation of the Sierra crest existed upstream of the mountains, characteristics often associated with severe downslope winds along the lee slopes (e.g., Durran 1990) and rotor circulations.

The Sierra Nevada is a continuous and narrow mountain range with a mean width of approximately 100 km and a length of 650 km. The geographical region of interest for the numerical simulation is focused on the Owens Valley, California, which is adjacent to the topography comprised of the main crest of the high Sierra to the west, with peaks over 4400 m elevation, that abruptly descends to the valley floor at

High-resolution simulations of rotors indicate the presence of small-scale vortices or subrotors embedded within the parent rotor. These subrotors, which in some respects are analogous to multiple suction vortices within a tornado, may pose the greatest hazard to aviation. Vortex stretching and tilting are likely to play an important role in the enhancement of vorticity within such subrotors, but these processes can play no role in changing the vorticity in a two-dimensional flow, such as that shown in Fig. 3.

To further examine the internal structure of rotors found in nature, a three-dimensional high-resolution real data simulation was carried out for a case of mountain waves on 28 and 29 October 2000 in the lee of the Sierra Nevada range. The GOES visible satellite image for 0000 UTC 29 October 2000, shown in Fig. 4, indicates numerous trapped mountain waves in the lee of the northern Sierra and a

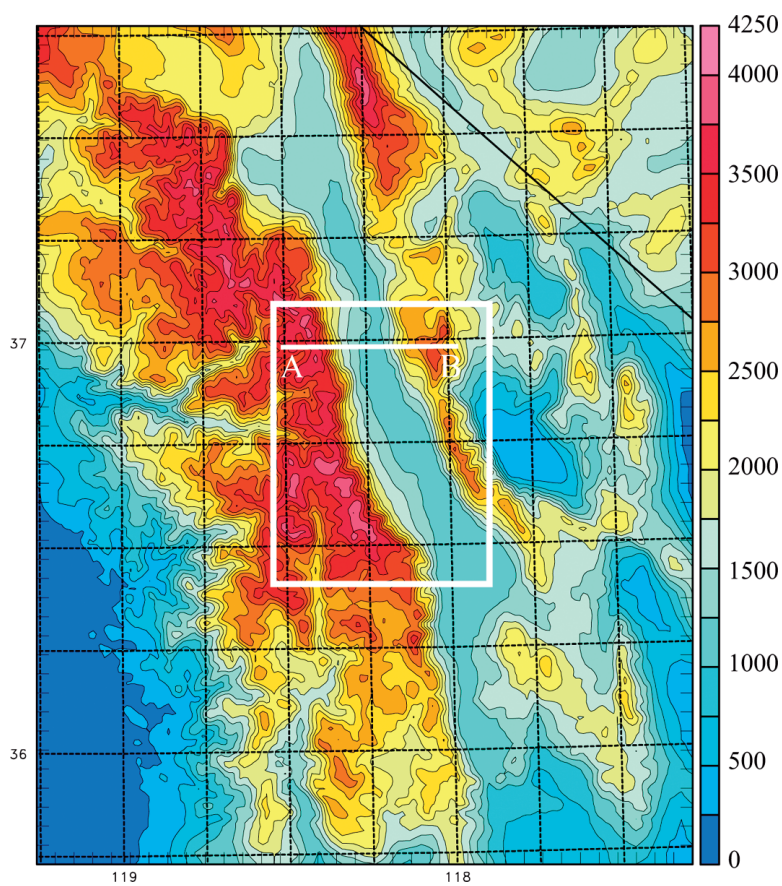

Fig. 6. Topography (m) for the fourth grid mesh (Δ*x* = 1 km) is shown by the color scale and contours every 250 m. The location of the fifth grid mesh (Δ*x* = 333 m) is represented by the white rectangle. The dashed latitude and longitude lines are shown every 0.25°.

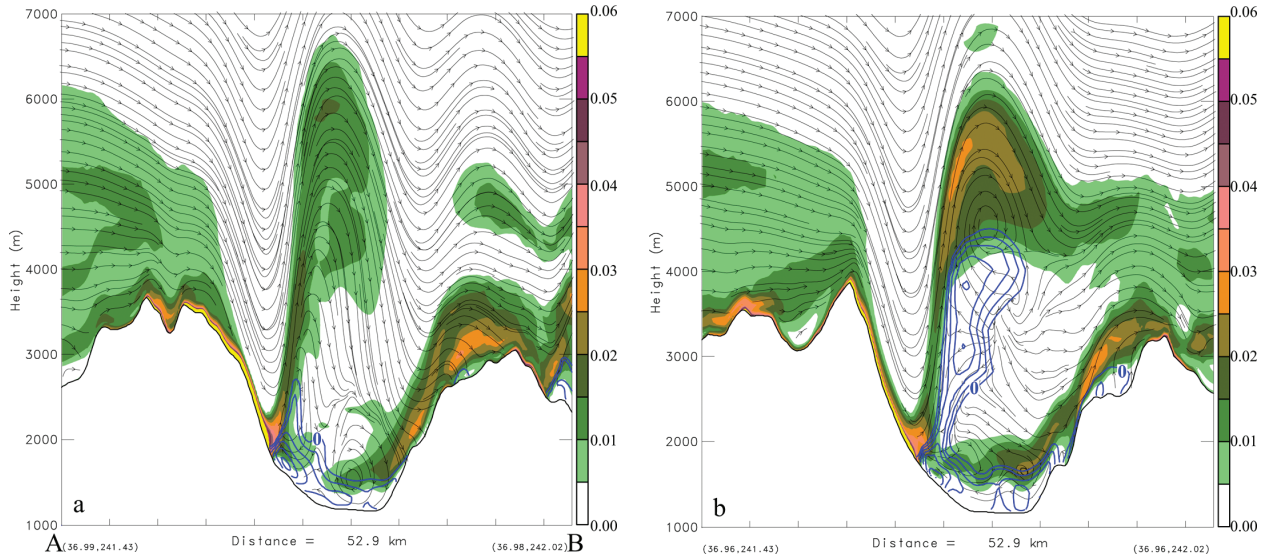

Fig. 7. Streamlines and horizontal vorticity (y-component) from a three-dimensional numerical simulation at the 12-h time valid at 0000 UTC 29 Oct 2000 for (a) along axis AB (see Fig. 6) and (b) approximately 3 km south of axis AB. The horizontal vorticity greater than 0.005 s^{-1} is shaded in color. The cross-mountain wind speed less than or equal to zero is shown using blue isotachs (every 1 m s^{-1}).

a mean elevation of 1200 m, as shown in Fig. 6. The eastern portion of the valley is bounded by the White and Inyo Mountains. Near Independence, California, the width of the Owens Valley is approximately 15 km.

The COAMPS model simulation is initialized at 1200 UTC 28 October 2000 using all available observations blended with a first guess based on the Navy Operational Global Atmospheric Prediction System, which is also used for lateral boundary conditions. In this application, the model makes use of five nested grid meshes centered on the Owens Valley, with the finest mesh using a 333-m grid increment (location shown in Fig. 6). A west–east oriented vertical cross section of streamlines and horizontal vorticity along line AB (Fig. 6) at the 12-h time valid at 0000 UTC 29 October 2000 is shown in Fig. 7a. Similar to the idealized two-dimensional simulation shown in Fig. 3, a sheet of large horizontal vorticity (*y*-component) is significantly enhanced in the boundary layer along the lee slopes of the Sierra range and lifted upward into the lee wave crest to near 7 km. Two small-scale circulations are present within the rotor near the surface, perhaps indicative of the role of three-dimensionality and the complex forcing associated with the upstream and downstream topography. The strong horizontal and vertical shears, particularly at the upstream edge of the rotor, generate intense turbulence that is advected into the upstream edge of the lee wave.

An indication of the along-ridge variation in the finescale structure within the rotor may be obtained by examining a second vertical cross section shown in Fig. 7b, which is located approximately 3 km to the south of that shown in Fig. 7a. The flow at 4 km in Fig. 7b is strongly reversed, with maximum speeds of 5 m s^{-1} that are more intense than the extremum in the reversed flow near the surface. The substantial variation in rotor substructure between the cross sections in Figs. 7a,b is consistent with the possibility that vortex stretching and tilting may play a role in amplifying any subrotors that do develop. The substructures shown in Figs. 7a,b are also highly transient, suggesting that a given area within the rotor can be relatively benign at one moment and extremely dangerous a few minutes later. Such localized regions of turbulence and shear within the parent rotor may be one of the key terrain-induced phenomena that contribute to an enhanced rate of aviation accidents in mountainous regions (e.g., Carney et. al 1995).

Guidance for forecasting rotors is virtually nonexistent despite their important and direct link to aviation safety issues. The general characteristics of rotors have been known since the completion of the Sierra Wave Project in the 1950s, yet surprisingly little is known about several of their key aspects, including their internal structure, strength, climatology, and microphysical processes. Recent numerical simulations suggest that the meteorological conditions favorable

for the formation of strong rotors are similar to those that favor the development of trapped lee waves and downslope winds, namely 1) a significant cross-mountain wind component of at least 10 m s^{-1}; 2) an elevated inversion near crest level; and 3) a significant increase in the cross-mountain wind speed above crest level. Nevertheless, more extensive theoretical and observational efforts are required to verify and refine these general guidelines. Forecasting of mountain-wave activity and associated turbulence in support of aviation operations are commonly performed using empirical and statistical techniques, which could be extended to include rotors if more sophisticated guidelines prove to be reliable.

In the five decades following the Sierra Wave Project, the characteristics and dynamics of rotors have remained an enigma. New observations of rotors, such as from the forthcoming Terrain-Induced Rotor Experiment (T-REX; Grubišić and Kuettner 2003), will be needed to gain insight into the characteristics of rotors, including their internal structure, and to evaluate the results from high-resolution and eddy-resolving numerical models to determine the predictability of rotors. The multiphase T-REX field campaign and high-resolution numerical model simulations should ultimately provide the means to substantially improve our understanding and ability to forecast mountain-wave induced rotors.

ACKNOWLEDGMENTS. The research support for the first author was provided by ONR PE0601153N. The support for the second author was provided by NSF Grants ATM-0137335 and ATM-0242980. Opinions expressed are those of the authors and not necessarily of NSF. COAMPS™ is a trademark of the Naval Research Laboratory. Computing time was supported in part by a grant of HPC time from the DoD MSRC at Vicksburg, Mississippi.

FOR FURTHER READING

Carney, T. Q., A. J. Bedard, J. M. Brown, M. J. Kraus, J. McGinley, T. A. Lindholm, 1995: *Hazardous Mountain Winds and Their Visual Indicators.* Department of Commerce/NOAA, 80 pp.

Doyle, J. D., and D. R. Durran, 2002: The dynamics of mountain-wave induced rotors. *J. Atmos. Sci.*, **59,** 186–201.

Durran, D. R., 1990: Mountain waves and downslope winds. *Atmospheric Processes over Complex Terrain, Meteor. Monogr.,* No. 45, Amer. Meteor. Soc., 59–81.

Grubišić, V., and J. P. Kuettner, 2003: Terrain-induced rotor experiment (T-REX). *10th AMS Conf. on Mesoscale Processes*, Portland, OR, Amer. Meteor. Soc., CD-ROM 11.3.

Hodur, R. M., 1997: The Naval Research Laboratory's Coupled Ocean/Atmosphere Mesoscale Prediction System (COAMPS). *Mon. Wea. Rev.*, **125,** 1414–1430.

Holmboe, J., and H. Klieforth, 1957: Investigations of mountain lee waves and airflow over the Sierra Nevada. Final Rep., Contract AF19(604)-728, University of California AD No. 133606, University of California, Los Angeles, Los Angeles, CA, 290 pp.

Kuettner, J., 1959: The rotor flow in the lee of mountains. GRD Research Note 6, Air Force Cambridge Research Laboratories, 20 pp.

Lester, P. F., and W. A. Fingerhut, 1974: Lower turbulent zones associated with mountain lee waves. *J. Appl. Meteor.*, **13,** 54–61.

Ludlam, F. H., and R. S. Scorer, 1957: *Cloud Study: A Pictorial Guide.* John Murray Ltd., 80 pp.

Queney, P., G. Corby, N. Gerbier, H. Koschmieder, and J. Zierep, 1960: The airflow over mountains. WMO Tech. Note No. 34, World Meteorological Organization, Geneva, Switzerland, 135 pp.

Whelan, R. F., 2000: *Exploring the Monster. Mountain Lee Waves: The Aerial Elevator.* Wind Canyon Books, 169 pp.